A Thresholdless Tunable Raman Nanolaser Using ZnO-graphene Superlattice

*By Haiou Zhu[1], Xintong Xu[1], Xiaoqing Tian[1], Jiaoning Tang[1], Huawei Liang[1], Lingling Chen[1] , Yi Xie[2] , Xiaodong Zhang[2], Chong Xiao[2], Ran Li[2], Qiao Gu[3], Ping Hua[4], and Shuangchen Ruan[1]**

[1] Dr H. O. Zhu, Dr X. T. Xu, Prof. X. Q. Tian, Prof. J. N. Tang, Prof. S. C. Ruan
College of Optoelectronic Engineering,
Shenzhen University,
Shenzhen, GuangDong, P. R.China.

[2] Dr. X. D. Zhang, Dr. C. Xiao, Dr. R. Li, Prof. Y. Xie
Hefei National Laboratory for Physical Sciences at Microscale,
University of Science & Technology of China,
Hefei, AnHui, P. R.China.

[3] Prof. Q. Gu
International Institute of Quantum Biology,
Haßloch, Germany.

[4] Prof. P. Hua
Optoelectronics Research Centre,
University of Southampton,
Southampton, UK.

Email: scruan@szu.edu.cn

Keywords: surface Plasmon; superlattice; graphene; nanolaser; Raman

Nanolasers based on surface plasmon opens up new platform for advanced nanophotonics technologies.[1-6] As Raman scattering process convert pump laser into new frequencies, so development of Raman nanolaser may allows for tunable nanolasers and boost the development of innovative nanophotonics technology. The Raman conversion for conventional Raman laser is intrinsically challenging as high intensities of the pump laser are required to drive the nonlinear effect. In recent years, miniaturization of Raman silicon laser has been successfully achieved with the assistance of reverse-biased p-i-n diode at centimeter size or photonics-crystal with high-quality-factor nanocavity at micrometer size.[7-9] However, for applications such as high-resolution medical imagings or on-chip optical communications, ‘ultimate’ nanolasers with scalable, thresholdless,

efficient source of radiation that operates at room temperature and occupies a small volume at nanometer size are highly desired,[10] which have not yet be realized by conventional methods for Raman laser. On the other hand, although nanolasers based on surface plasmon amplification by stimulated emission of radiation (SPASER) have been proposed and experimentally demonstrated making use of surface plasmon polaritons to dramatically shrink the optical mode volume for sub-diffraction confinement of light.[11] Raman nanolaser based on surface plasmon have not been reported since most of the Raman vibration modes are indistinctly enhanced for surface enhanced Raman scattering effect. For Raman nanolaser, development of new materials that can enhance the specific Raman vibration modes and suppress the undesired ones is required.

In searching for an ideal material for tunable Raman nanolasing, we turn to a new class of graphene-based superlattice. As is known, among the surface plasmon materials, graphene possesses highly tunable intrinsic plasmon and strong confinement on optical modes but a fairly small interaction cross-section with light,[12,13] and the working frequency of surface plasmon is mainly in the mid-infrared to microwave regions, in which region it is difficult to find a gain medium. A promising way is to introduce extremely high dopant in graphene by making graphene-based hybrids. Besides noble metals and graphene, doped semiconductors such as doped ZnO are promising options for sub-diffractional confinement of light.[14-16] A key advantage of doped semiconductors is that the plasmon frequencies are tunable in a wide range with varied doping level. For atomic-scale hybrid heterorstructure, the rich physics at interface of the hybrid heretostructure enable novel tunable optics for effective subdiffractional confinement of light[17-21] Here we report the growth of ZnO-graphene superlattice via a spatially confined reaction method.[22] We demonstrate room-temperature thresholdless tunable Raman lasing in freestanding ZnO-graphene superlattice, covering the near-infrared to visible wavelength region with varied pump laser. A new mechanism-“Selective Surface Plasmon Amplification by Stimulated Raman Scattering (SSPASRS)” is proposed responsible for generation of Raman nanolaser.

The superlattices were prepared via a spatially confined reaction method (the method section), in which zinc compounds grow in the interlayer of few-layered reduced graphene oxides (abbreviate as RGO). The structure of the superlattice was confirmed by means of X-ray diffraction (XRD), high resolution transmission electron microscopy (HRTEM) and selected area electron diffraction (SAED) pattern, respectively. The X-ray diffraction pattern in **Figure 1a** indicated that the as-obtained material was a laminated structure with interlayer distance of 10.6Å (001), and diffraction peaks at about 5.3Å and 3.53Å could be assigned to second and third order diffraction of (001), thus defined as (002) and (003) respectively. The HRTEM images in **Figure 1b** with inter planar distance of 2.81Å and the lattice point distance of 1.87Å revealed that the phase on the surface of the as-obtained material is wurtzite-type ZnO[23,24]. The HRTEM image in **Figure 1c** further comfirmed that the interlayer distance is 10.6Å, and the lattice plane distance of 2.48Å and 2.81Å within the interlayer of 10.6Å could be assigned to (101) and (100) lattice plane of ZnO layer. The d-spacing of the diffraction spots A, B, C, D, E in the hexagonal symmetry SAED pattern in **Figure 1d** are calculatedto be 1.48 Å, 1.91 Å, 2.48 Å, 2.81Å and 3.53 Å, respectively, among them diffraction spot A, B, C, D can be assigned to (103), (102), (101), (100) lattice plane of the ZnO layer, and the diffraction spot E with the d-spacing 3.53Å could be assigned to third order diffraction of the interlayer distance (001) of the superlattice. The XRD pattern and HRTEM images confirmed that the as-obtained material is superlattice consisting of ZnO and graphene.The interlayer distance 10.6Å is roughly the sum of graphene and ZnO layers. Based on this information, the proposed structure of the superlattice is presented in Figure 1a and 1b, the superlattice is constructed with alternating stacked graphene and ZnO layer. The Raman spectra shown in **Figure 2a** further confirmed the existence of ZnO and graphene in the superlattice.

The lasing spectra of the freestanding ZnO-graphene superlattice were measured with the pump laser from 488nm to 785nm at a pump power of 1mW. There are four peaks marked as (E_1, E_2, E_3, E_4) in each lasing spectrum with the same relative intensity as shown in **Figure 2b-f**. Calculated results on the wave-number

shifts of the four laser signals in Supplementary Table S1, S2 shows that the wave-number shifts between the pump photon and the emitted photon is constant whatever the pump lasers are used, which indicate a typical feature of Raman nanolaser. Furthermore, the wave-number shifts of the four laser signals in Figure 2b-f is roughly coincident with the Raman shifts of the four vibration modes in ZnO marked as V_1, V_2, V_3, V_4 respectively in Figure 2a, which confirmed that the lasing signals marked E_1-E_4 in Figure 2b-f are Raman nanolasing corresponding to the V_1-V_4. The energy sketch map of Raman scattering process is given in **Figure 2g.**

The lasing spectra under different pump power densities by a CW semiconductor diode laser at 514.5nm are shown in **Figure 3a**, and the detail spectra of individual lasing signal are see supplementary Figure S1. The light-light (L-L) plot in **Figure 3b** shows the output power of the four lasing mode (E_4-E_4) as a function of pump power at room temperature, which follows straight lines with no pronounced kink, which confirmed thresholdless lasing hypothesis.[25] The corresponding peak linewidth with different pump power intensity are given in **Figure 3c,** the peak linewidths of the four lasing are narrower than 0.35nm, and the linewidth of the strongest lasing signal is about 0.07nm, indicating extreme monochromaticity of the four lasing peaks. The temperature-dependent lasing spectra presented in **Figure 3d** shows that the lasing behavior is coincident from room temperature to 80K. The thresholdless behavior is further manifested in the linewidth spectra in **Figure 3e**, where narrow, Lorentzian-like emissions of E_4-E_4 are obtained over the entire range of pump power from the first signal detected above the detection system noise flow at 3μW to the highest pump power of 2.752mW.

The dynamic behavior is further studied by careful study of linewidth behavior. At low pump levels, the linewidth shown in Figure 3c is almost constant, and does not narrow with increased pump power, implying that the linewidth shows no subthreshold behavior.[25-27] Then at high pump levels, the linewidth is broaden with increased pump power. The spectral broaden may be the result of many factors such as the new frenquency component arising from the nonlinear effect, and the spectrally-varying loss to the fundamental

field in the stimulated Raman scattering process, which is interpreted in Supplementary Text S1.[28,29] A first-principle Maxell-Bloch formulation of light-matter interaction are used to inverstigate the dynamics of nanolasers through quantum electrodynamics,[30] and the dynamics of Raman nanolaser in graphene-based superlattice are to be investigated via this approach in the future work.

Although roughly coincident, the wave-number shift calculated from Figure 2b-f and wave-number shifts in supplementary Table. S1, S2 are slightly smaller than the Raman shift in Figure 2a (202cm^{-1}, 330cm^{-1}, 743cm^{-1} and 1105cm^{-1} for V_1-V_4 respectively) with roughly the same amplitude of variation, indicating red-shift of the Raman scattered photons in the following enhance/propagate process. This red-shift of the Raman scattered photon arises from the photon-induced charge transfer process within the superlattice as manifested in supplementary Figure S2. The charge transfer process can be explained by the calculated result on electronic structure of ZnO-graphene superlattice in supplementary Figure S3. Graphene are calculated to has a tiny band gap of 15 meV, and the highest occupied molecular orbital (HOMO) and lowest unoccupied molecularorbital (LUMO) of ZnO are asymmetrically disposed on both sides of the Fermi level of graphene. Photo-induced charge transfer can be easily excited within the ZnO-graphene superlattice. The red-shift of the Raman scattered photon are explained in supplementary Figure S4.

The charge transfer process leads to carrier distribution between ZnO and graphene. The electronic structure calculation in Figure S3 shows that, in a unit structure consisting of 4×4 graphene on the top of a 3×3 ZnO (0001) surface with 6 atomic layers, graphene transfer 0.8 electron to ZnO layer, and the carrier intensity in ZnO is about $9.1\times10^{20}/cm^3$, which is high enough to support surface plasmon[14,31]. Surface plasmon may be excited in the interface of graphene and ZnO layer since when semiconductors are heavily doped, metallic-like optical properties such as surface plasmons may appear due to the metallic behavior arising from the many-electron effect controlled through the free electron density.[14,16] Kretschmann configuration is used for optical coupling of surface plasmons (**Figure 4a**). In this study, the wavelength-scanning mechanism, which

is similar to that proposed by Johansen[32] are used to detect the surface plasmon. A p-polarized white light was incident on a prism surface at an angle when light are totally reflected. **Figure 4b** shows the variation in reflectance ratio (R_1/R_0) as a function of the incident wavelength corresponding to a fixed incident angle of 50˚, (R_1 and R_0 are the reflectivity when the bottom of the prism is coated with and without ZnO-graphene superlattice, respectively). The curves are obtained by a fourth-order polynorminal fit of the experimental data supplementary Figure S5. The broad dip in the reflectivity ratio curve represents the resonance that occurs when the momentum of the incoming light matches with the momentum of the surface plasmons in ZnO-graphene superlattice. The result shows that there are two surface plasmon resonance peaks in ZnO-graphene superlattice, indicating that there are two surface plasmon modes which resonant with the incident light at different wavelength. Surface plasmons can greatly diminished the mode volume of the Raman scattering light, and amplify the scattered light by orders of magnitude in the near-infrared to visible range.

There are several Raman active vibration modes in Figure 2a, among them four vibration modes marked V_1-V_4 are selectively enhanced. Selective surface plasmon amplification by stimulated Raman scattering (SSPASRS) are proposed as the mechanism for Raman nanolaser. As is known, the intensity of Raman scattering dependents on the differential scattering cross section,[33,34] which is proportional to the Raman scattering factor S_P, where:

$$S_P = 45\left(\frac{\partial \alpha_P}{\partial Q_P}\right)^2 + 7\left(\frac{\partial \gamma_P}{\partial Q_P}\right)^2 \qquad (1)$$

α_P and γ_p are the isotropic and anisotropic polarization tensor. The change of polarization tensor leads to the variation of the Raman scattering intensity. Surface plasmon is collective oscillation of the conduction electrons, electron-density oscillate perpendicular to the plane of the interface as shown in **Figure 4c**. In the superlattice, atomic-thick gain medium ZnO layers are uniformly localized in the interior of the conducting medium, and are localized perpendicular to the oscillate direction of the electron-density. Therefore the polarization tensor perpendicular to the interface is rapidly, periodically changed at a resonance frequency of

surface plasmon. The Raman vibration modes perpendicular to the interface will be selectively enhanced according to periodically changing polarization tensor[35], and Raman vibration modes parallel to the interface will be suppressed since there are almost no components of the electron-density oscillation parallel to the interface. That is the reason for the selective enhancement of the Raman vibration modes for multi-mode Raman nanolaser.

In summary, Raman nanolaser based on selective surface plasmon amplification by stimulated Raman scattering (SSPASRS) is proposed and experimental demonstrated with ZnO-graphene superlattice. The special geometry, in which atomic-thick gain medium are in the interior of the conducting medium of surface plasmon, is crucial for highly directional preferred selection of Raman vibration modes for thresholdless Raman nanolaser. This Raman nanolaser allows for tunable nanolaser from visible to near-infrared range at room temperature. The Raman nanolaser not only substantially expands the available range of nanolaser, but also boosts the development of advanced nanophotonics technologies such as high-resolution medical imagings and on-chip optical communications.

Experimental Section

Synthesis of ZnO-graphene superlattice: The ZnO-graphene superlattices were synthesized via a spatially confined reaction method, the monolayered ZnO grow in the interlayers of reduced graphene oxides (RGO). Firstly, graphene oxide (abbreviated as GO) is prepared via a modified Hummer's method,[36] then graphene oxide was deoxidized by hydrazine hydrate (85 %) and ammonia solution (25 %) to reduced graphene oxide (RGO). Then the RGO solution was obtained for the following use: 0.2 mmol zinc acetylacetonate and 0.8 ml H_2O_2 were dissolved into 30 ml acetone, then 1mmol RGO solution was dropped into the solution, magnetic stirring for several minutes and ultrasonicated for about half an hour to intercalate the zinc oxide groups homogenously into the interlayer of adjacent RGO nanosheets. Then the well-distributed suspension was

transferred into 40 ml stainless Teflon-lined autoclave followed by solvothermal process at 210°C for 36 hours. When cooled to room temperature in air, the product was collected and washed with distilled water and ethanol, and dried in vacuum at 60 °C for 8 hours.

*Structural characterizations***:** The X-ray diffraction was performed in Bruker D8 Advance. The high resolution transmission electron microscopy and selected area electron diffraction (SAED) pattern are performed in field emission FEI-F20 operated at 200 kV. The Raman spectra and lasing spectrum are performed in raman evolution hr800.

Calculation:The calculations are performed within the Vienna ab initio simulation package (VASP).[37] The Perdew–Burke–Ernzerhof[38] generalized gradient approximation is used. The electron-ion interaction is described by PAW method[39]. 29.40 Ry is used as the plane wave basis set cutoff.

Optical properties measurement: The Raman spectrum and the lasing spectrum are performed in Raman evolution hr800 of Horiba company. The pump laser is provided by Argon-Krypton ion laser. The lasing spectra are measured with freestanding ZnO-graphene superlattice on single crystalline Silicon.

Acknowledgements

We grateful acknowledge support from National Natural Science Foundation of China (No: 51502175, No:61575129 and No. 11304206) and Science & Technology Innovation Committee Foundation of Shenzhen (2014(1677)).

Received: ((will be filled in by the editorial staff))
Revised: ((will be filled in by the editorial staff))
Published online: ((will be filled in by the editorial staff))

[1] Y. J. Lu, J. Kim, H. Y. Chen, C. Wu, N. Dabidian, C. E. Sanders, C. Y. Wang, M. Y. Lu, B. H. Li, X. Qiu, W. H. Chang, L. J. Chen, G. Shvets, C, K, Shih, S. Gwo, *Science* **2012**, *337*, 451.

[2] S. F. Wu,s. Buckley, J. R. Schaibley, L. F. Feng, J. Q. Yam, D. G. Mandrus, F. Hatami, W. Yao, J. Vuckovic, A. Maiumdar, X. D. Xu. *Nature* **2015**, *520*,69 .

[3] M. A. Noginov, G. Zhu, A. M. Belgrave, R. Bakker, V. M. Shalaev, E. E. Narimanov, S. Stout, E. Herz,

T. Suteewong, U. Wiener, *Nature* **2009**. *460*,1110.

[4] R. F. Oulton, V. J. Sorger, T. Zentgraf, R. M. Ma, C. Gladden, L. Dai, G. Bartal, X. Zhang, *Nature* **2009**, *461*,629.

[5] R.-M. Ma, R. F.Oulton, V. J. Sorger, G. Bartal, X. Zhang, *Nat. Mater*. **2011**, *10*,110.

[6] F. H. L. Koppens, D. E. Chang, F. J. G. Abajo, *Nano Lett***. 2011**,*11*,1130.

[7] H. S. Rong, R. Jones, A. Liu, O. Cohen, D. Hak, A. Fang, M. Paniccia. *Nature* **2005**, *433*, 725.

[8] H. S. Rong, S. Xu, Y. H. Kuo, V. Sih, O. Cohen, O. Raday, M. Paniccia, *Nat. photon*. **2007**,*1*,232.

[9] Y. Takahashi, Y. Inui, M. Chihara, T. Asano, R. Teeawaki, S. Noda, *Nature* **2012**, *237*, 450.

[10] S. Noda, *Science* **2006**, *314*, 260.

[11] J. S. T. Gongora, A. E. Miroshnichenko, Y. S. Kivshar, A. Fratalocchi, *Laser Photonics Rev*. **2016**,*10*, 432.

[12] F. H. L. Koppens, D. E. Chang, F. J. G. Abajo, *Nano Lett*. **2011**,*11*,1130.

[13] R. R. Nair, P. Blake, A. N. Grigorenko, K. S. Novoselov, T. J. Booth, T. Stauber, N. M. R Peres, A. K. Geim, *Science* **2008**, *320*, 1308.

[14] G. V. Naik, J. J. Liu, A. V. Kildishev, V. M. Shalaev, A. Boltasseva, *PNAS* **2012**, *109*, 8834

[15] H. Kim, M. Ssofsky, S. M. Prokes, O. J. Glembocki, A. Pique, *Appl. Phys. Lett*. **2013**, *102*,171103.

[16] V. N. T. Guilengui, L. Cerutti, E. Rodriguez, E. Tournie, T. Taliercio, *Appl. Phys. Lett*. **2012**, *101*, 161113.

[17] R. F. Oulton, V. J. Sorger, D. A. Genov, D. A. Pile, X. Zhang, *Nat. Photon***.2008**, *2*, 495.

[18] R. F. Oulton, V. J. Sorger, T. Zentgraf, R. M. Ma, C. Gladden, L. Dai, G. Bartal, X. Zhang, *Nature* **2009**, *461*,629.

[19] S. Dai, Q. Ma, M. K. Liu, T. Andersen, Z. Fei, M. D. Goldflam, M. Wagner, K. Watanabe, T. Taniguchi, M. Thiemens, G. C. A. M. Janssen, S. E. Zhu, P. Jarilli-Herrero, M. M. Fogler, D. N. Basov, *Nat. Nanotech.* **2015**, *10***,** 682.

[20] T. A. Woessner, M. B. Lundeberg, Y. Gao, A. Principi, P. A.lonso-Gonzalez, M. Carrega, K. Watanabe, T. Taniguchi, G. Vignale, M. Poloni, J. Hone, R. Hillenbrand, F. H. L. Koppens, *Nat. Mater.* **2014**, *14***,** 421.

[21] J. D. Caldwell, I. Vurgaftman, J. G. Tischler, O. J. Glembocki, J. C. Owrutsky, T. L. Reinecke, *Nat. Nanotech*. **2016**, *11*,9.

[22] H. O. Zhu, C. Xiao, H. Cheng, F. Grote, X. D. Zhang, T. Yao, Z. Li, C. M. Wang, S. Q. Wei, Y. Lei, Y. Xie, *Nat. Commun.***2014**, *5*, 3960.

[23] S. C. Adrahams, J. L. Bernsten, *Acta.Cryst. B* **1969**, *25*,1233.

[24] R. Cuscó, E. Alarcón-Lladó, J. Ibáñez, L. Artús, *Phys. Rev.* B **2007**, *75*, 165202.

[25] M. Khajavikhan, A. Simic, M. Katz, J. H. Lee, B. Slutsky, A. Mizrahi, V. Lomakin, Y. Fainman, *Nature* **2012**, *482*, 204.

[26] A. L.Schawlow, C. H. Townes, *Phys. Rev*.**1958**, *112*,1940.

[27] G. K. A. Björk, Y. Yamamoto, *Appl.Phys. Lett.***1992**, *60*, 304.

[28] G. P. Agrawal, Nonlinear Fiber Optics, University of Rochester, Unites States,**2001**.

[29] G. M. Bonner, J. Lin, A. J. Kemp, J. Wang, H. Zhang, D. J. Spence, H. M. Pask, *Opt. Express* **2014**, *22*, 7492.

[30] A. Fratalocchi, C. Conti, G. Ruocco, *Phys. Rev. A* **2008**, *78*, 013806.

[31] V. N. Guilengui *et al*, *Appl.Phys. Lett*. **2012**, *101*, 161113.

[32] K.Johansen, H. Arwin, I.LundstrÖm, B. Liedberg, *Rev. Sci. Instrum*.**2000**, *71*, 3530.

[33] J. R. Ferraro, K. Nakamoto, C. W. Brown, Introductory Raman Spectroscopy, *Academic Press: Amesterdam and Boston*,**2003**.

[34] J. Neugebauer, M. Reiher, C. Kind, B.A. Hess, *J. Comput. Chem*. **2002**, *23*, 895.

[35] D. M. Basko, S. Piscanec, A. C. Ferrari, *Phys. Rev. B* **2009**, *80*,165413.

[36] S. William, J. R. Hummers, E. Offeman, *J. Am. Chem. Soc*. **1958**, *80*,1339

[37] G. Kresse, & J. Furthmiiller, *Comput. Matter. Sci*. **1996**, *6*, 15.

[38] J. P. Perdew, K. Burke, M. Ernzerhof, *Phys. Rev. Lett.***1996**, *77*, 3865.

[39] Kresse, G.&Joubert, D. *Phys. Rev. B* **1999**, *59*, 1758._

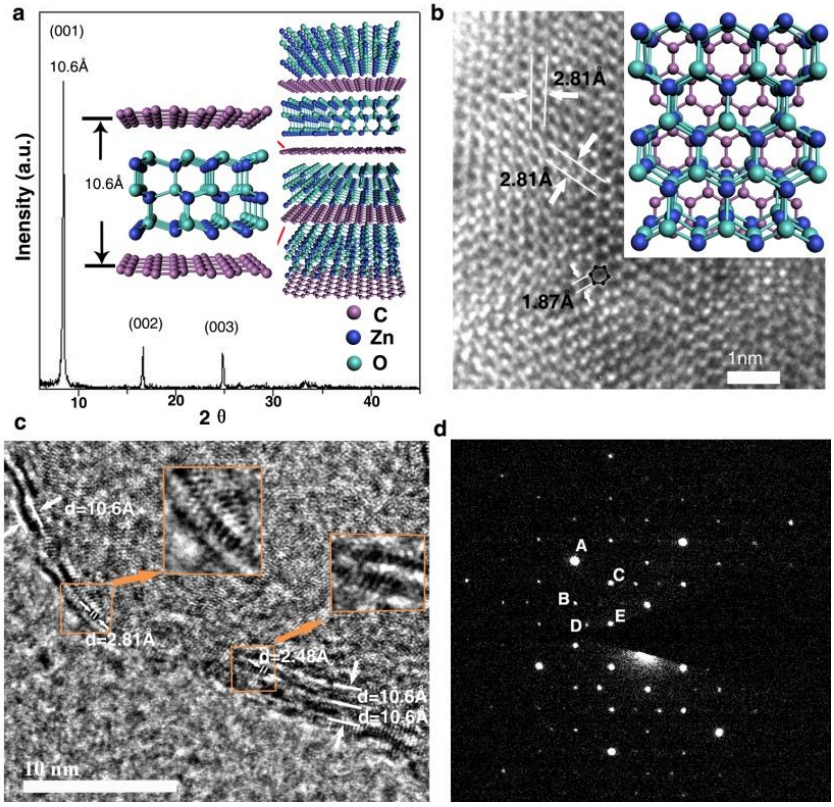

Figure 1. a) The calculated XRD pattern (pink line) and the experimental XRD pattern (black line) of the superlattice, the inner image is the sketch map of the structure. **b)** HRTEM image of the basal plane of the superlattice nanosheets, the d-spacing of 2.81Å and the side length of 1.87Å measured from the hexatomic ring of the HRTEM image can be assigned to ZnO layer. insert：The sketch map of the basal plane of the superlattice. **c)** HRTEM image of the cross-section edge of the superlattice nanosheets. **d)** The SAED pattern of the superlattice.

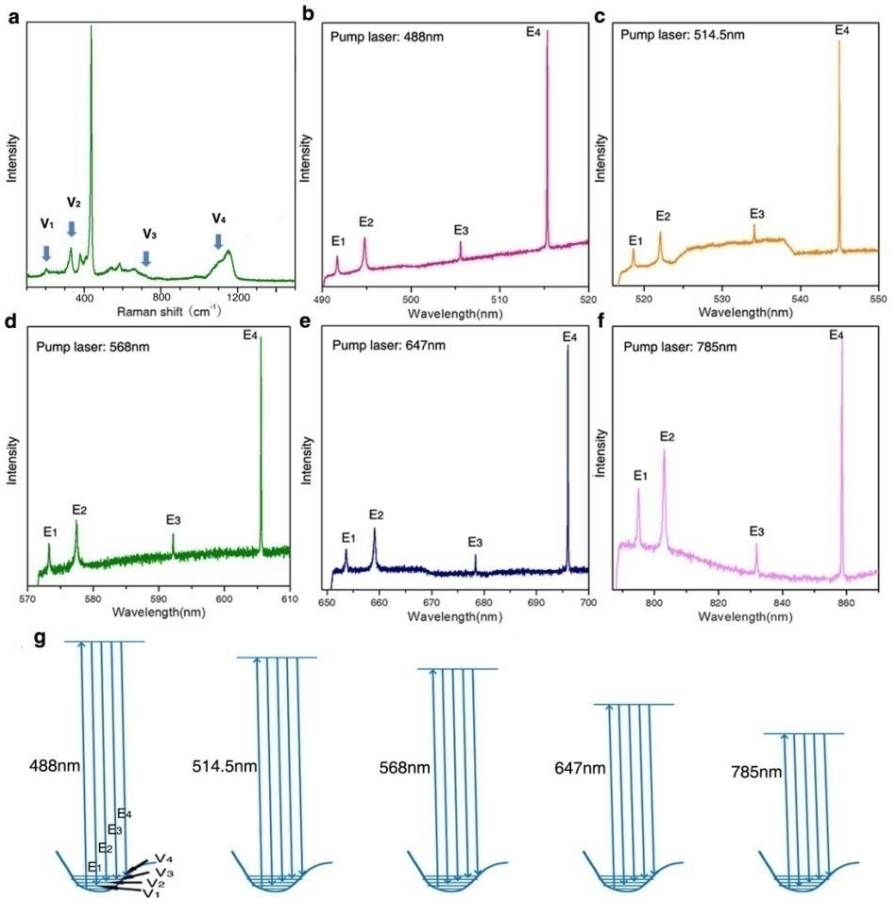

Figure 2. a) the Raman spectra of the ZnO. The lasing spectra of ZnO-graphene superlattice with incident laser wavelength of **b)** 488nm, **c)** 514.5nm, **d)** 568nm, **e)** 647nm and **f)** 785nm at a pump power of 3.2kW/cm^2, **g)** The energy sketch map of Raman scattering process, vibration modes V_1-V_4 correspond to V_1-V_4 in (a), the four scattered photons in each of sketch map correspond to the Raman laser signals E_1-E_4 in (b-f)

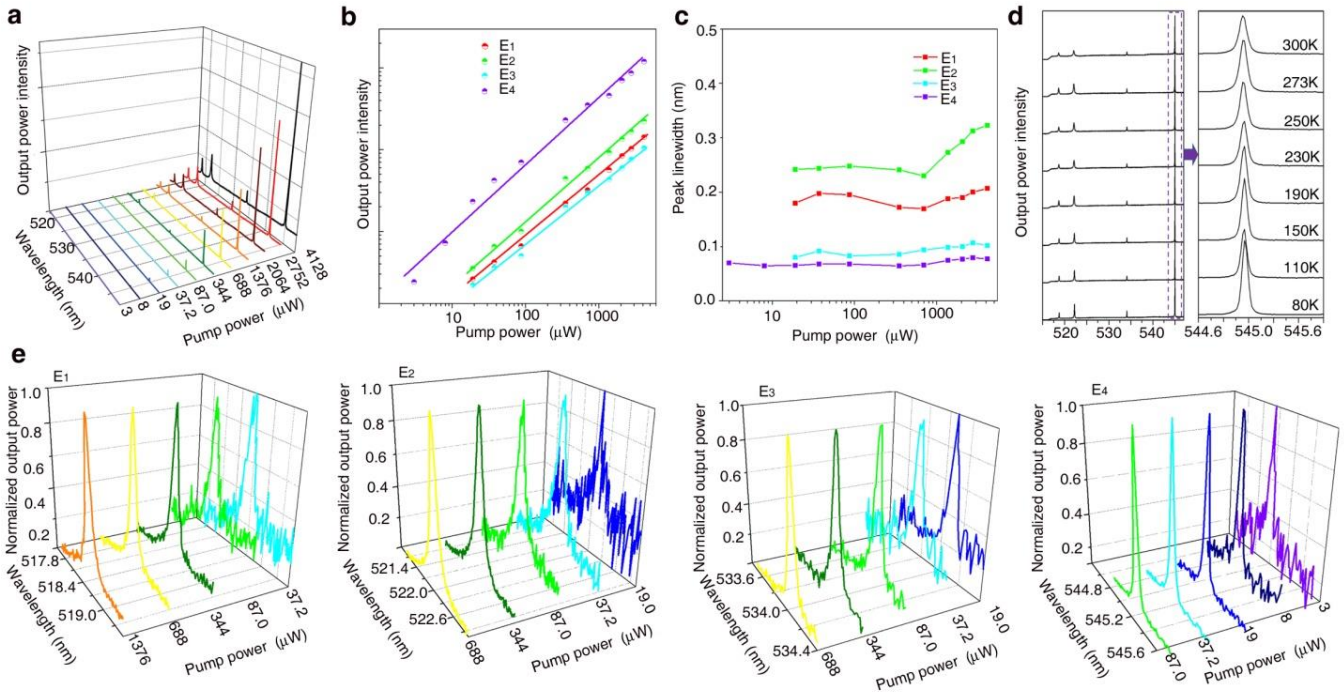

Figure 3. a) The lasing spectra pumped by a CW-514.5nm semiconductor diode laser with different pump power intensity. **b)** The light-light curve for the lasing peaks E_1-E_4. **c**) The linewidth of the lasing peaks E_1-E_4. **d)** Temperature-dependent lasing behavior from 80K to 300K. e) The lasing spectra for lasing peaks E_1-E_4 respectively.

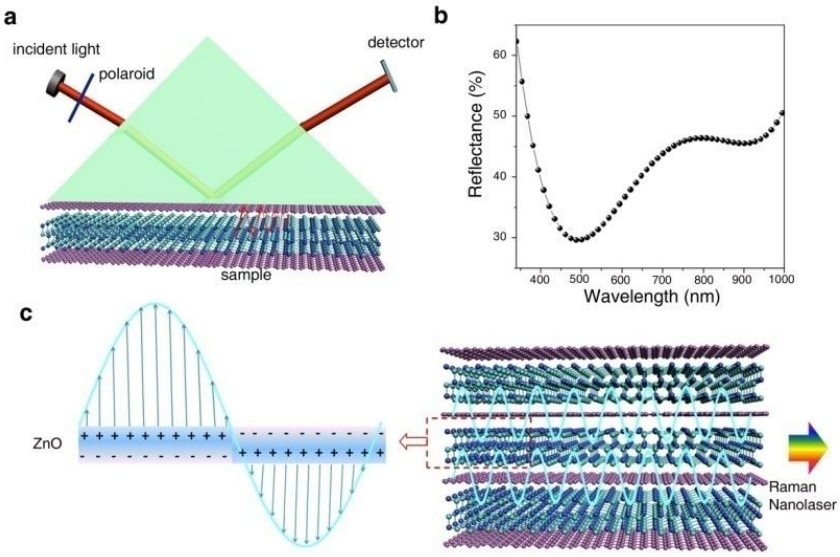

Figure 4. a) the schematic of surface plasmon resonance in ZnO-graphene superlattice using Kretschmann configuration. **b)** the surface plasmon resonance reflectivity spectrum of ZnO-graphene superlattice using Kretschmann configuration, it is a fourth-order polynomial fit to the experimental data (Supplementary Fig. S4). **c)** the highly directional preferred selection of Raman vibration modes for thresholdless Raman nanolaser in ZnO-graphene superlattice.

The table of contents entry

Experimental data reveal that ZnO-graphene superlattice is synthesised via a spatially confined reaction method. When illuminated by pump laser, the stokes photons of the superlattice could be greatly amplified by the surface plasmon at the interface of graphene and ZnO. The special geometry of ZnO-graphene superlattice allows for highly directional preferred selection of Raman vibration modes for multi-mode Raman nanolaser. Benefiting from these, the Raman nanolaser allows for tunable nanolaser from visible to near-infrared range at room temperature.

Keyword: surface Plasmon; superlattice; graphene; nanolaser; Raman

*Haiou Zhu[1], Xintong Xu[1], Xiaoqing Tian[1], Jiaoning Tang[1], Huawei Liang[1], Lingling Chen[1] , Yi Xie[2] , Xiaodong Zhang[2], Chong Xiao[2], Ran Li[2], Qiao Gu[3], Ping Hua[4], and Shuangchen Ruan[1]**

Thresholdless Tunable Raman Nanolaser Using ZnO-graphene Superlattice

ToC Figure